

Asymmetry in endogenously bridged binuclear copper(II) and zinc(II) complexes formed by 1,2-bis[1,4,7-triazacyclonon-1-yl]propan-2-ol†

Fiona H. Fry,^a Boujemaa Moubaraki,^a Keith S. Murray,^a Leone Spiccia,^{*a} Mark Warren,^a Brian W. Skelton^b and Allan H. White^b

^a School of Chemistry, Monash University, Victoria 3800, Australia

^b Chemistry Department, University of Western Australia, Crawley, W.A., 6009, Australia

Received 20th November 2002, Accepted 23rd December 2002

First published as an Advance Article on the web 3rd February 2003

Endogenously bridged binuclear copper(II) and zinc(II) complexes of singly deprotonated 1,2-bis[1,4,7-triazacyclonon-1-yl]propan-2-ol (T_2PrOH) have been prepared by reacting the ligand hexabromide salt with appropriate metal salts. An X-ray structural analysis of the Cu(II) complex, $[Cu_2(T_2PrO)Br_2]Br \cdot 2H_2O$ (**1**), confirmed the presence of a complex cation, $[Cu_2(T_2PrO)Br_2]^+$, which consists of Cu(II) centres linked by an endogenous alkoxo bridge. Three N donors from the tacn macrocycle and a bromo ligand complete the coordination sphere. The two Cu(II) centres are in slightly different distorted square pyramidal (*SPY*) Cu(II) geometries. A magnetic susceptibility study of **1** revealed the presence of moderately strong antiferromagnetic coupling between the Cu(II) centres ($J = -86 \text{ cm}^{-1}$), as found for other binuclear Cu(II) complexes bridged by endogenous alkoxo groups. The molecular structure of the Zn(II) complex, $[Zn_2(T_2PrO)Br(H_2O)_2](ClO_4)_2$ (**2**), apart from confirming that the two Zn(II) were bridged by an endogenous alkoxo group, revealed coordination asymmetry in the two Zn(II) centres. One Zn(II) centre is six-coordinate and pseudo-octahedral with the coordination sphere occupied by three tacn nitrogens, the bridging oxygen, one bromo and one water ligand, while the other is five-coordinate and pseudo-square pyramidal, lacking the bromo ligand.

Introduction

Copper and zinc complexes of the tridentate macrocycle, 1,4,7-triazacyclononane (tacn), multiple tacn assemblies and N-functionalised derivatives of these ligands continue to be explored in a variety of contexts.^{1–5} The use of these ligands in the assembly of bridged polynuclear copper(II) complexes has contributed to the development of magnetostructural correlations for exchange interactions in such complexes.^{6–10} In most of these complexes, exogenous groups bridge the metal centres. By comparison, few polynuclear complexes of tacn derivatives have been isolated which have endogenous bridging between two or more copper or zinc centres.^{11,12} We report here the synthesis and characterization of endogenously bridged Cu(II) and Zn(II) complexes incorporating the deprotonated form of the binucleating ligand, 1,2-bis[1,4,7-triazacyclonon-1-yl]propan-2-ol (T_2PrOH). For the Cu(II) complex, the combination of an X-ray structure analysis and magnetic study has enabled the ability of the endogenous alkoxo bridge to mediate magnetic exchange to be examined. In the Zn(II) complex, an alkoxo bridge also connects the Zn(II) centres, but in this case coordination asymmetry is evident as five- and six-coordinate metal centres co-exist within each binuclear unit.

Results and discussion

Preparation of complexes

The Cu(II) complex of the T_2PrOH ligand was prepared by reacting aqueous solutions of $T_2PrOH \cdot 6HBr$ and $CuBr_2$ (1 : 2 ratio) and appropriate adjustment of pH. Blue crystals of $[Cu_2(T_2PrO)Br_2]Br \cdot 2H_2O$ (**1**) deposited on slow evaporation of the blue solution. For the Zn(II) complex, $T_2PrOH \cdot 6HBr$ was dissolved in water and, after the pH was adjusted to 7, added to an aqueous solution of $Zn(ClO_4)_2 \cdot 6H_2O$. Following work-up,

$[Zn_2(T_2PrO)Br(H_2O)_2](ClO_4)_2$ (**2**) precipitated as colourless crystals on slow evaporation. The IR spectrum of **1** shows bands at 3335, 3290 and 3216 cm^{-1} while **2** has a band at 3331 cm^{-1} which can be ascribed to $\nu(NH)$ stretches of the secondary amines in the ligand. $\nu(OH)$ stretches due to coordinated water or water in the crystal lattice are evident at 3463 (**1**) and 3460 (**2**) cm^{-1} . For **1**, of the structures that are consistent with the microanalysis (*viz.*, $[M_2(T_2PrO)Br_n(H_2O)_m]^{(3-n)+}$; $m = 0–2$; $n = 0–3$; $m + n = 2–4$), the X-ray structure established that the complex cation has two coordinated bromides, *viz.*, $[Cu_2(T_2PrO)Br_2]^+$ (see below). The molar conductivities of **1** and **2** indicate that the coordinated bromides are substituted on dissolution forming $[M_2(T_2PrO)(H_2O)_m]^{3+}$. The electrospray mass spectrum of **2** exhibited peaks at m/z 643.1 and 623.1 which correspond to $\{Zn_2(T_2PrO)(ClO_4)_2\}^+$ and $\{Zn_2(T_2PrO)Br(ClO_4)\}^+$, respectively.

The 1H NMR spectrum of **2** (Fig. 1(a)), shows three multiplets at 2.77, 2.94 and 3.14 ppm due to the tacn methylene protons, a multiplet at 3.91 ppm due to the CH in the bridge and two signals for the two bridge methylenes, one seen as a triplet at 2.41 ppm and the second hidden under a signal due to the tacn methylene protons (7 and 7' in Fig. 1(a)). These signals compare well to those of the Zn(II) complex of the 2-methylpyridyl functionalised T_2PrOH .¹² The ^{13}C NMR spectrum of **2** (Fig. 1(b)) shows six signals in the 41–53 ppm region, indicating six different environments for the tacn ring carbons, and two signals due to 61.93 and 64.46 ppm due to the bridge carbons, as was found by Brudenell *et al.*¹² Thus, in solution at room temperature, the two halves of the complex are equivalent on the NMR timescale and coordination asymmetry, as found in the crystal structure (see below), is not apparent.

Crystal structures

The results of the single crystal X-ray structure determinations are consistent with the formulations of **1** and **2** as $[Cu_2LBr_2]Br \cdot 2H_2O$ and $[Zn_2LBr(OH_2)_2](ClO_4)_2$, respectively; in each case one formula unit, containing a binuclear cation (Fig. 2), and devoid of crystallographic symmetry, comprises the asymmetric

† Electronic supplementary information (ESI) available: Table S1 presenting selected ligand skeletal torsion angles. See <http://www.rsc.org/suppdata/dt/b2/b211490a/>

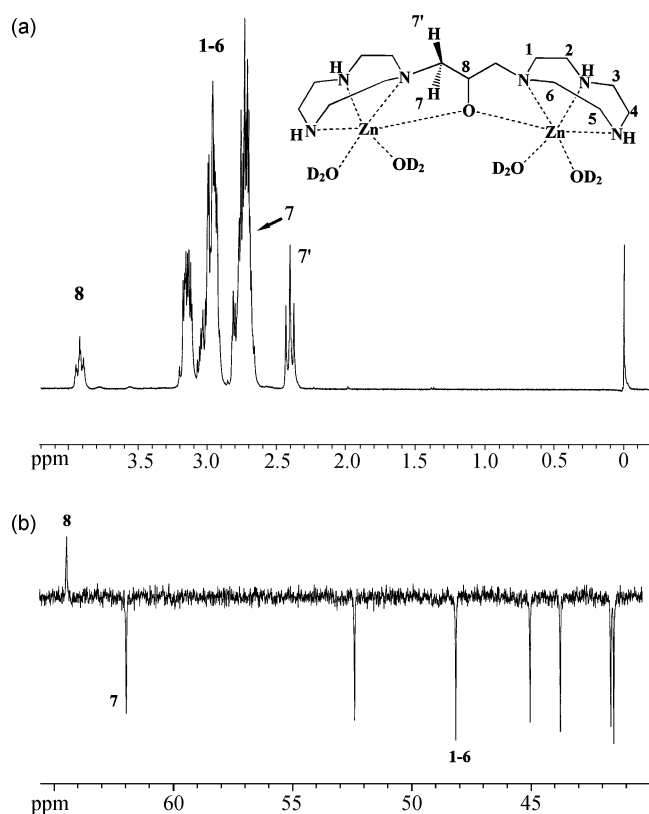


Fig. 1 ^1H (a) and ^{13}C (b) NMR spectra of **2**.

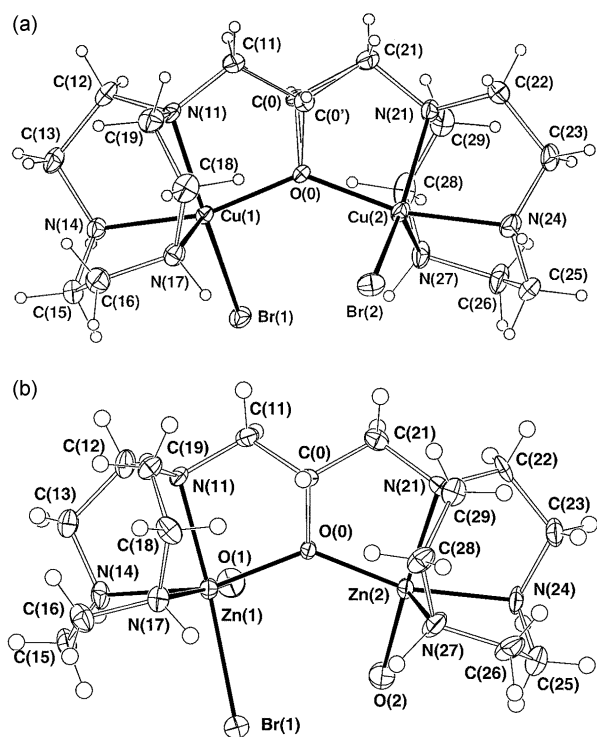


Fig. 2 Projections of the cations of the (a) Cu (**1**) and (b) Zn (**2**) complexes.

unit of the structure. The oligodentate ligand, comprised of two similar halves about the central C–O bond, embraces one metal atom within each half with the (anionic) oxygen atom bridging them. Each half of the ligand occupies four coordination sites about the metal with the three nitrogen atoms of the tacn ring facial in the coordination sphere (Table 1). The remainder of the metal coordination spheres are occupied by bromo or aqua ligands such that the overall formulations

for the two cations are $[\text{BrCuLCuBr}]^+$ and $[(\text{H}_2\text{O})\text{BrZnLZn}(\text{OH}_2)]^{2+}$, respectively.

The coordination spheres of Cu(1), Cu(2) and Zn(2) are five-coordinate and can be described as quasi-square pyramidal (*SPY*) with an axially ligated secondary amine nitrogen (N(27)). The electronic spectrum of the Cu(II) complex supports this geometric assignment (*vide infra*). Application of the geometric analysis of five-coordinate complexes of Rao and coworkers, leads to the conclusion that Cu(1) and Zn(2) are closer to *SPY* ($\tau = 0.02$ for both) than Cu(2) ($\tau = 0.28$).¹³ For **2**, this and other geometric features indicate that the binuclear cation has two copper atoms lying in distinct environments (Table 1). For example, a shift towards *TBPY* geometry for Cu(2) is indicated by a wider N(apical)–Cu–Br angle ($125.9(2)$ *cf.* $110.0(1)^\circ$ about Cu(1)) and by the fact that the N(21)–Cu(2)–Br(2) angle ($149.1(2)^\circ$) is more acute than the corresponding angle about Cu(1) ($164.4(2)^\circ$). In contrast to most quasi-*SPY* Cu(II) complexes of bis(tacn) ligands, in which a tertiary bridgehead nitrogen is in the apical position,^{8–10} the endogenous alkoxy bridge in **2** forces a secondary nitrogen into the apical position. Remarkably, the differences in coordination environment are more pronounced in the zinc cation where the second metal atom Zn(1) is six- rather than five-coordinate, a further water molecule entering that coordination sphere, with a concomitant increase in the other M–L distances. Although small-sized polynuclear zinc(II) complexes exhibiting coordination asymmetry are relatively rare,^{14–17} such a feature is not uncommon among the active sites of zinc enzymes.¹⁸

The ligand conformations are of considerable diversity and interest, causing small but significant differences in the angular parameters (see electronic supplementary information †). In the copper complex, the two halves of the ligand are similar, and of the same chirality, so that the ligand overall (and cation), has quasi-2 symmetry. Attainment of overall-2-symmetry is thwarted by the differences in the metal atom environments mentioned above, also because the central carbon atom of the ligand C(0,0') is not trigonal planar but tetrahedral, so that the hydrogen disposition to one side or the other of the ambient

Table 1 Selected cation geometries in **1** and **2**

M/segment(<i>n</i>)/X	Cu/1/Br	Cu/2/Br	Zn/1/Br ^a	Zn/2/O(H ₂)
Distances (Å)				
M(<i>n</i>)–O(0)	1.931(4)	1.930(4)	2.018(4)	1.971(5)
M(<i>n</i>)–N(<i>n</i> 1)	2.087(3)	2.088(5)	2.198(5)	2.138(6)
M(<i>n</i>)–N(<i>n</i> 4)	2.015(6)	2.018(6)	2.144(5)	2.131(6)
M(<i>n</i>)–N(<i>n</i> 7)	2.195(6)	2.175(7)	2.166(6)	2.112(6)
M(<i>n</i>)–X(<i>n</i>)	2.425(1)	2.432(1)	2.621(1)	2.067(5)
Angles (°)				
M(<i>n</i>)–O(0)–M(<i>n</i>)	136.2(2)		135.1(2)	
M(<i>n</i>)–O(0)–C(0), (0')	106.8(8), 115.7(8)	116.2(7), 106.5(8)	112.2(4)	112.7(4)
M(<i>n</i>)–N(<i>n</i> 1)–C(<i>n</i> 1)	105.4(3)	105.8(4)	103.3(4)	102.5(3)
M(<i>n</i>)–N(<i>n</i> 1)–C(<i>n</i> 2)	103.7(5)	102.6(4)	103.1(4)	106.2(4)
M(<i>n</i>)–N(<i>n</i> 1)–C(<i>n</i> 9)	109.4(4)	108.0(5)	109.1(4)	107.8(4)
C(<i>n</i> 1)–N(<i>n</i> 1)–C(<i>n</i> 2)	113.4(5)	114.2(6)	114.0(5)	114.5(5)
C(<i>n</i> 1)–N(<i>n</i> 1)–C(<i>n</i> 9)	112.6(7)	112.4(6)	113.4(5)	112.3(5)
C(<i>n</i> 2)–N(<i>n</i> 1)–C(<i>n</i> 9)	111.7(5)	112.9(5)	112.8(5)	112.6(5)
M(<i>n</i>)–N(<i>n</i> 4)–C(<i>n</i> 3)	111.8(5)	111.2(4)	110.6(4)	110.4(4)
M(<i>n</i>)–N(<i>n</i> 4)–C(<i>n</i> 5)	105.9(4)	106.0(5)	103.6(4)	101.5(5)
C(<i>n</i> 3)–N(<i>n</i> 4)–C(<i>n</i> 5)	114.4(5)	113.8(6)	114.0(6)	113.7(5)
M(<i>n</i>)–N(<i>n</i> 7)–C(<i>n</i> 6)	107.6(5)	108.5(6)	110.2(4)	109.0(4)
M(<i>n</i>)–N(<i>n</i> 7)–C(<i>n</i> 8)	101.3(4)	101.3(5)	105.6(4)	102.4(4)
C(<i>n</i> 6)–N(<i>n</i> 7)–C(<i>n</i> 8)	114.8(5)	113.8(5)	113.3(6)	114.2(6)
O(0)–M(<i>n</i>)–X(<i>n</i>)	96.1(1)	95.9(1)	99.9(1)	99.0(2)
O(0)–M(<i>n</i>)–N(<i>n</i> 1)	83.9(2)	82.4(2)	82.7(2)	85.0(2)
O(0)–M(<i>n</i>)–N(<i>n</i> 4)	164.2(2)	165.9(2)	159.2(2)	163.7(2)
O(0)–M(<i>n</i>)–N(<i>n</i> 7)	105.7(2)	99.3(2)	109.6(2)	104.4(2)
X(<i>n</i>)–M(<i>n</i>)–N(<i>n</i> 1)	165.4(2)	149.1(2)	170.0(1)	162.8(2)
X(<i>n</i>)–M(<i>n</i>)–N(<i>n</i> 4)	93.4(2)	94.1(2)	97.8(2)	90.8(2)
X(<i>n</i>)–M(<i>n</i>)–N(<i>n</i> 7)	110.0(1)	125.9(2)	88.8(2)	109.9(3)
N(<i>n</i> 1)–M(<i>n</i>)–N(<i>n</i> 4)	83.7(2)	83.9(2)	81.8(2)	82.0(2)
N(<i>n</i> 1)–M(<i>n</i>)–N(<i>n</i> 7)	83.9(2)	84.6(2)	81.3(2)	85.0(2)
N(<i>n</i> 4)–M(<i>n</i>)–N(<i>n</i> 7)	82.8(2)	82.7(3)	81.6(2)	84.2(2)

^a Zn(1)–O(1) is 2.290(5) Å, O(1)–Zn–O(0), N(11,14,17), Br(1) are 85.9(2), 97.9(2), 82.6(2), 164.1(4), 91.9(1)°.

'plane' in the complex is incompatible with 2-symmetry. In fact, 2-symmetry is achieved at the gross level by disorder in this C–H moiety, the structure being a superimposed composite of the two contributing systems.

The ligand disorder noted in **1** is absent in **2**, the zinc counterpart. Here, however, the ligand symmetry is quite different, being a good approximation to *m* overall, compatible with an achievable non-disordered ligand conformation, but broken in the cation more widely by the impact of the differences (again) in the metal coordination environments. Thus while the individual cation in **1** is inherently chiral, because of the ligand disposition, that of **2** is only so by virtue of the different zinc coordination environments. As well as the torsion angles being opposite in sign, divergences between 'equivalent' parameters of the ligand in **2** are greater than in **1** (see electronic supplementary information †). In the copper complex cation, Br(1) ⋯ H(27), Br(2) ⋯ H(17) are 2.7₄, 3.0₁ Å, with Br(*n*) ⋯ H(*n*4) 3.0₃, 2.9₉ Å; the environments of the ligated bromides are predominantly filled by other longer Br ⋯ H_N contacts. The Br(1) ⋯ Br(2) separation is 4.540(2) Å. The interaction voids seem to be loosely occupied by the remaining bromide ion and solvent water molecules with relatively high displacement amplitudes. In **2**, the most interesting inter-species interaction involves the association of the anions with the zinc(II) cation, anion 1 anchored by O(11) ⋯ H(17), O(13) ⋯ H(27) 2.2₄, 2.2₃ Å, side by side, and anion 2 by O(21) ⋯ H(14) (*x* – 1/2, 3/2 – *y*, *z* – 1/2) 2.1₇ Å.

One consequence of the single oxygen M–O–M bridge is that the M ⋯ M distance is quite short (3.582(1) and 3.684(1) Å for **1** and **2**, respectively). Sessler *et al.*¹⁹ have found that an oxo- and hydroxo-bridged tetranuclear iron cluster incorporating the same ligand exhibits M ⋯ M separations of 3.510(2) and 3.513(2) Å for the endogenously bridged units, that are only slightly shorter than those in **1** and **2**. In fact, the M ⋯ M separations in **1** and **2** are typical for Cu(II) and Zn(II)

complexes that are bridged by an endogenous alkoxo bridge, including some complexes that contain additional multiatom bridges (*e.g.*, see Table 2 and refs. 15–17).

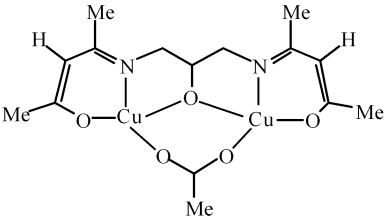
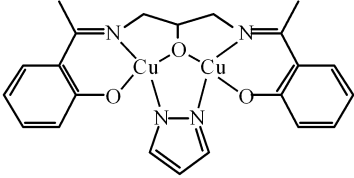
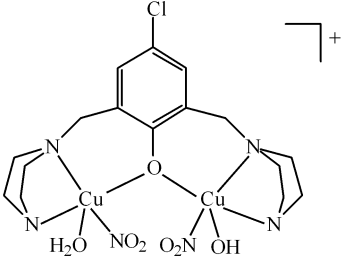
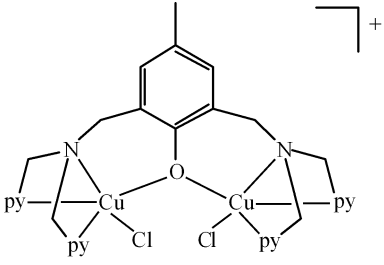
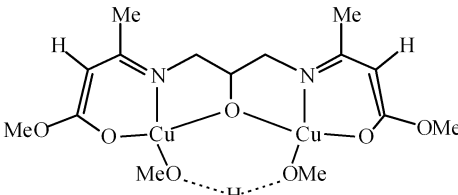
Electronic spectra

The solution electronic spectrum of **1** exhibits maxima at 689 and 1072 nm which are typical for Cu(II)–tacn complexes with pseudo-*SPY* Cu(II) geometry, rather than *TBPY* and are due to $d_{z^2} \rightarrow d_{x^2-y^2}$ and $d_{yz} \rightarrow d_{x^2-y^2}$ transitions.²⁰ The position of these bands, which for *SPY* Cu(II) complexes are typically found at 650 and 1050 nm, indicates significant distortion towards *TBPY* (λ_{\max} can be as high as 720 nm²¹ for very distorted *SPY* Cu(II) complexes while *TBPY* complexes generally show one band in the 800–900 nm range²²). A shift in the main band from 689 to 631 nm for the solid state spectrum indicates a solid state geometry closer to *SPY*.

Magnetic and EPR properties

The finding that the room-temperature magnetic moment for **1** is a little reduced from the range normally expected for mononuclear copper(II) complexes led to a variable temperature magnetic study. Magnetic susceptibilities of **1** were determined in a field of 1 T over the temperature range of 300–4.2 K. The plots are shown in Fig. 3. The variable temperature magnetic moment plot shows a steady decrease in magnetic moment from 1.57 μ_B (per Cu) at 300 K to 0.05 μ_B at 4.2 K, which is indicative of moderate strength antiferromagnetic coupling between the copper(II) centres. The small increase in the magnetic susceptibility observed at low temperatures is due to a trace of monomeric impurity, which is a feature of complexes possessing antiferromagnetic interactions between the metal centres.²³ The data were fitted to a modified Bleaney–Bowers equation (eqn. (1)) calculated for two *S* = 1/2 centres under a $-2JS_1 \cdot S_2$ spin Hamiltonian, using a non-linear least squares fitting

Table 2 Comparison of Cu–O–Cu bond angles, Cu ··· Cu distances and *J* values for alkoxo bridged binuclear copper(II) complexes

Complex	Cu ··· Cu/Å	Cu–O–Cu°	<i>J</i> /cm ⁻¹	Ref.
[Cu ₂ (T ₂ PrO)Br ₂][Br·2H ₂ O (1)	3.582(1)	136.2(2)	-86	This work
	3.502(2)	133.3(3)	-83	24
	3.359(4)	125.1	-120	25
	3.603(4)	130.1(6)	-122	26
	4.128(3)	140.2(5)	0	27
	3.644(2)	137.7(5)	-318	24

^a py = 2-Pyridyl.

routine. The susceptibility equation (eqn. (1)) allows for a monomeric impurity seen commonly in such systems, assuming the *g*-value is the same as that for the complex.

$$\chi_{\text{Cu}} = \frac{Ng^2\beta^2}{kT} \left[3 + \exp\left(\frac{-2J}{kT}\right) \right]^{-1} (1-P) + \frac{Ng^2\beta^2 P}{4kT} + N_a \quad (1)$$

The parameters obtained on fitting of the data were *g* = 2.01, *J* = -86 cm⁻¹ and *P* = 0.0012. The value of *J* can be compared to other 2-propanolato or phenolato bridged complexes, most of which have a second (or even third) exogenous bridge such as OAc⁻ or pyrazolate (see Table 2).²⁴⁻²⁷ A complex with a single alkoxo bridge as part of a Schiff-base ligand, together with an H-bonded link (MeO–H ··· OMe) displays very strong coupling, *J* = -318 cm⁻¹.²⁴ The Cu–O–Cu bridge angle of

137.7(5)° compares well to the present 136.2(2)°. Such large angles and corresponding Cu ··· Cu separations normally lead to very strong antiferromagnetic coupling²⁴ and thus the smaller *J* value for **1** needs explanation. Normally the “end groups” (acac, sal, tacn, N(CH₂py)₂, halide) play a minor part in the net *J* value when they lead to unusual geometries around each Cu with consequent effects on the Cu “magnetic orbitals” used in the bridging pathways (*e.g.* *J* = 0 for the Cl-complex shown in Table 2 because the PhO⁻ bridge is in the apical (*z*) position relative to Cu (d_{x²-y²}) magnetic orbitals²⁷). More important is the nature of the Cu(II) orbitals (*i.e.* d_{x²-y²}) for planar or *SPY* geometry and their coplanarity and bridging geometry (Cu–O–Cu) relative to the RO⁻ (or PhO⁻) bridging atom. The more coplanar, the more negative is the *J* value. Smaller dihedral angles between the Cu *SPY* basal planes, which incorporate the RO⁻ (or PhO⁻) bridging oxygen, lead to

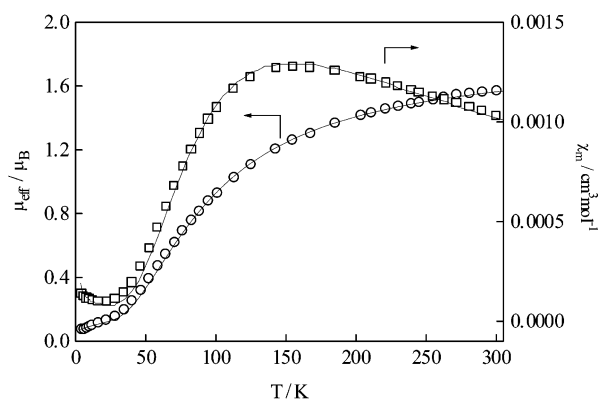


Fig. 3 Plot of μ_{eff} (per Cu) and χ_m (per Cu) versus temperature for complex **1**.

smaller J values (see nitro derivative in Table 2²⁶). Other features such as non-trigonal O(bridging) geometry²⁶ and the presence of exogenous bridges (counter-complementarity effects^{24,27}) will also reduce the antiferromagnetic coupling. In **1**, a dihedral angle of $76.35(8)^\circ$ shows that the SPY basal planes of each Cu(II) are not coplanar and this leads to a diminution in the size of J relative to other μ -alkoxo (only) systems.²⁴ For the nitro (phenolate bridged) complex, a dihedral angle of 83.7° results in a lower than expected J value (-122 cm^{-1}) (see Table 2).

An X-band EPR spectrum of **1**, recorded at 77 K in frozen DMF–toluene solution, gave a very weak signal that was difficult to distinguish from the cavity signal of the instrument. This is not unexpected given the medium strength $\text{Cu}^{\text{II}} \cdots \text{Cu}^{\text{II}}$ coupling seen in the susceptibility plots although, in principle, a triplet state line should be visible at 77 K for such a J value.

Experimental

Materials

Commercial reagents and solvents were of reagent grade quality or better were used as received. $\text{T}_2\text{PrOH}\cdot 6\text{HBr}$ was prepared by the method of Wieghardt *et al.*²⁸

Physical measurements

^1H and broad band decoupled ^{13}C NMR spectra were recorded in D_2O on either a Bruker AC200, BrukerDPX300 or Bruker DRX400 spectrometer using an internal standard of sodium (2,2,3,3,3- d_4 -3-(trimethylsilyl)propionate (TMSP-D). Electrospray ionization (ESI) mass spectra were recorded on a Micro-mass Platform quadrupole mass spectrometer or a Bruker BioApex 47e Fourier Transform mass spectrometer. Quoted m/z values refer to the most intense peak present in each signal envelope. IR spectra were recorded using KBr disks on a Perkin-Elmer 1600 series FTIR spectrophotometer. Solution and solid state diffuse reflectance UV-Visible-NIR spectra of **1** were measured on a Cary 5G instrument. The room-temperature magnetic moment of **1** was measured on a Faraday balance which incorporated a four-inch Newport electromagnet fitted with Faraday-profile pole faces. Variable temperature magnetic susceptibilities were measured on a Quantum Design MPMS Squid magnetometer over a temperature range of 4.2 to 300 K, in a field of 10 kG (1 T). Samples were contained in calibrated gelatine capsules and held in the centre of a drinking straw fused to the end of the sample rod. The temperature and field were checked against a standard Pd sample and $\text{CuSO}_4\cdot 5\text{H}_2\text{O}$. The data was fitted with the POLYMER non-linear least squares program written at Monash University. The EPR spectrum of **1** was measured at 77 K in a 1 : 1 DMF–toluene mixture on a Varian E12 spectrometer operating at X-band frequency (9.1 GHz). Solution conductivity was measured using a

Crison 522 Conductimeter with Pt black electrodes calibrated with 0.020 M KCl solution.

Syntheses

[Cu₂(T₂PrO)Br₂]Br·2H₂O (1). $\text{T}_2\text{PrOH}\cdot 6\text{HBr}$ (0.30 g, 0.38 mmol) was dissolved in water (10 ml) and the pH was adjusted to 6 with 1 M NaOH. A solution of $\text{Cu}(\text{ClO}_4)_2\cdot 6\text{H}_2\text{O}$ (0.56 g, 1.5 mmol in 5 ml of water) was added. During the addition the pH dropped to *ca.* 3. The pH was increased to 10 with 1 M NaOH, the $\text{Cu}(\text{OH})_2$ that formed was removed and the pH re-adjusted to 7 with HCl. The solution was allowed to stand and after *ca.* 2 weeks blue crystals of **1** had formed. These were collected by *vacuum* filtration, washed with MeOH and air-dried. Yield, 0.17 g (63%).

Analyses. Found: C 25.0, H 5.1, N 11.4%. Calc. for $\text{Cu}_2\text{C}_{15}\text{H}_{37}\text{N}_6\text{O}_3\text{Br}_3$: C 25.2, H 5.2, N 11.7%. UV-Vis-NIR spectrum: solid ($\lambda_{\text{max}}/\text{nm}$): 631, 1081; solution (H_2O ; $\lambda_{\text{max}}/\text{nm}$ ($\epsilon/\text{M}^{-1} \text{cm}^{-1}$): 270 (6291), 689 (252), 1072 (50). IR spectrum (KBr; ν/cm^{-1}): 3463s, 3335m, 3290s, 3216m, 2942s, 2896s, 2848s, 1738w, 1648w, 1613w, 1455s, 1380m, 1357m, 1283w, 1242w, 1155w, 1110s, 1087s, 1010s, 987m, 927m, 900m, 870m, 844m, 820m, 776m, 748w, 687w, 569w, 543w, 504w. Magnetic moment: μ_{eff} (per Cu) = $1.56 \mu_{\text{B}}$ at 300 K. EPR spectrum: g_{\parallel} 2.27, A_{\parallel} $161 \times 10^4 \text{ cm}^{-1}$, g_{\perp} 2.05. Molar conductivity (H_2O): $400 \text{ S cm}^2 \text{ mol}^{-1}$.

[Zn₂(T₂PrO)(H₂O)₂Br](ClO₄)₂ (2). Compound **2** was synthesised by dissolving $\text{T}_2\text{PrOH}\cdot 6\text{HBr}$ (0.15 g, 0.19 mmol) in 5 ml water, adjustment of the pH to *ca.* 7 with 1 M NaOH and addition of this solution to an aqueous solution of $\text{Zn}(\text{ClO}_4)_2\cdot 6\text{H}_2\text{O}$ (0.28 g, 0.75 mmol, in excess). The pH of the filtrate was taken to 10 and any precipitate that formed was removed by filtration. The pH of the colourless filtrate was adjusted to 7 with 1 M HBr and the solution volume reduced by heating on a steam bath. After one week at room temperature colourless crystals deposited that were suitable for X-ray crystallography. The crystals were collected, washed with acetone and air-dried. Yield, 58 mg (41%).

Analyses. Found: C 24.2, H 5.1, N 11.1%. Calc. for $\text{Zn}_2\text{C}_{15}\text{H}_{37}\text{N}_6\text{O}_8\text{Cl}_2\text{Br}$: C 23.7, H 4.9, N 11.1%. IR spectrum (KBr, ν , cm^{-1}): 3460s br, 3331s, 2940m, 2891m, 1628w, 1490m, 1460m, 1364w, 1104m, 1094vs, 933m, 907m, 885m, 817w, 623s. ^1H NMR (D_2O): δ 2.41 (t, 2H, CH_2 bridge), 2.77 (10H, m, CH_2 tacn and 2H, CH_2 bridge), 2.94 (10H, m, CH_2 tacn), 3.14 (4H, m, CH_2 tacn) 3.91 (1H, m, CH bridge). ^{13}C NMR (D_2O): δ 41.04 (CH_2 tacn), 41.18 (CH_2 tacn), 43.33 (CH_2 tacn), 44.62 (CH_2 tacn), 47.81 (CH_2 tacn), 52.14 (CH_2 tacn), 61.93 (CH_2 bridge), 64.46 (CH bridge). Molar conductivity (H_2O): $390 \text{ S cm}^2 \text{ mol}^{-1}$. ESI mass spectrum (H_2O -MeOH) (m/z): 643.1 $\{\text{Zn}_2(\text{T}_2\text{PrO})(\text{ClO}_4)_2\}^+$; 623.1 $\{\text{Zn}_2(\text{T}_2\text{PrO})\text{Br}(\text{ClO}_4)\}^+$.

Structure determinations

Full spheres of CCD area-detector diffractometer data were measured (Bruker AXS instrument, ω -scans, monochromatic Mo-K α radiation ($\lambda = 0.71073 \text{ \AA}$), $2\theta_{\text{max}} = 58^\circ$, $T \text{ ca } 300 \text{ K}$ ($M = \text{Cu}$), *ca.* 153 K ($M = \text{Zn}$)). $N_{\text{(total)}}$ reflections were measured merging to N unique (R_{int} cited) after 'empirical'/multiscan absorption correction (proprietary software), N_{o} with $F > 4\sigma(F)$ being used in the full matrix least squares refinements. Anisotropic thermal parameter forms were refined for the non-hydrogen atoms, ($x, y, z, U_{\text{iso}}\text{H}$) being constrained at estimated values (where feasible). Conventional residuals R, R_w on $|F|$ are quoted at convergence (weights: $(\sigma^2(F) + 0.0004F^2)^{-1}$). Neutral atom complex scattering factors were employed within the Xtal 3.7 program system.²⁹ Pertinent results are given below and in the Tables and Figures, the latter showing 50% (153 K) or 20% (300 K) probability displacement envelopes for the non-hydrogen atoms, hydrogen atoms having arbitrary radii of 0.1 \AA .

Crystal/refinement data. $[\text{Cu}_2\text{LBr}_2]\text{Br}\cdot 2\text{H}_2\text{O} \equiv \text{C}_{15}\text{H}_{37}\text{Br}_3\text{-Cu}_2\text{N}_6\text{O}_3$, $M = 716.3$. Triclinic, space group $P\bar{1}$ (C_1^1 , No. 2), $a = 7.438(1)$, $b = 13.326(2)$, $c = 13.812(3)$ Å, $\alpha = 64.635(2)$, $\beta = 78.858(3)$, $\gamma = 89.469(3)^\circ$, $V = 1209$ Å³. D_c ($Z = 2$ f.u.) = 1.96_g cm^{-3} . $\mu_{\text{Mo}} = 67 \text{ cm}^{-1}$; specimen: $0.55 \times 0.30 \times 0.16$ mm; $T'_{\text{min,max}} = 0.37, 0.89$. $N_t = 13565$, $N = 5844$ ($R_{\text{int}} = 0.068$), $N_o = 4201$; $R = 0.054$, $R_w = 0.061$.

Comment. Hydrogen atoms associated with the (putative) water molecule oxygen atoms were not located. Disorder was resolvable in $\text{C}(0)$, $\text{C}(0) \cdots \text{C}(0')$ $0.66(3)$ Å.

$[\text{Zn}_2\text{LBr}(\text{OH}_2)_2](\text{ClO}_4)_2 \equiv \text{C}_{15}\text{H}_{37}\text{BrCl}_2\text{N}_6\text{O}_{11}\text{Zn}_2$, $M = 759.1$. Monoclinic, space group $P2_1/n$ (C_{2h}^5 , No. 14, variant), $a = 11.804(1)$, $b = 10.5204(9)$, $c = 21.619(2)$ Å, $\beta = 96.445(2)^\circ$, $V = 2668$ Å³. D_c ($Z = 4$ f.u.) = 1.89_g cm^{-3} . $\mu_{\text{Mo}} = 36 \text{ cm}^{-1}$; specimen: $0.20 \times 0.16 \times 0.12$ mm; $T'_{\text{min,max}} = 0.62, 0.86$. $N_t = 56052$, $N = 7023$ ($R_{\text{int}} = 0.054$), $N_o = 5691$; $R = 0.070$, $R_w = 0.12$.

Comment. Water molecule hydrogen atoms were not located. Significant difference map residues in the vicinity of $\text{Zn}(1)$, $\text{Br}(1)$ suggested possible cocrystallization of a minor isomeric component (such as might be obtained by substitution of water for Br, e.g.) but meaningful modelling was not feasible.

CCDC reference numbers 198150 and 198151.

See <http://www.rsc.org/suppdata/dt/b2/b211490a/> for crystallographic data in CIF or other electronic format.

Acknowledgements

This work was supported by the Australian Research Council. F. H. F. was the recipient of an Australian Postgraduate Award. We thank Dr S. Drew for conducting the EPR measurements.

References

- 1 W. B. Tolman, *Acc. Chem. Res.*, 1997, **30**, 227.
- 2 R. I. Haines, *Rev. Inorg. Chem.*, 2001, **21**, 165.
- 3 I. A. Fallis, *Annu. Rep. Prog. Chem., Sect. A*, 2002, **98**, 321; I. A. Fallis, *Annu. Rep. Prog. Chem., Sect. A*, 2001, **97**, 331; I. A. Fallis, *Annu. Rep. Prog. Chem., Sect. A*, 1999, **95**, 313.
- 4 L. F. Lindoy, *Adv. Inorg. Chem.*, 1998, **45**, 75.
- 5 E. L. Hegg and J. N. Burstyn, *Coord. Chem. Rev.*, 1998, **173**, 133.
- 6 L. Spiccia, B. Graham, M. T. W. Hearn, G. Lazarev, B. Moubaraki, K. S. Murray and E. R. T. Tiekink, *J. Chem. Soc., Dalton Trans.*, 1997, 4089.
- 7 P. Chaudhuri, D. Ventur, K. Wieghardt, E. M. Peters, K. Peters and A. Simon, *Angew. Chem., Int. Ed. Engl.*, 1985, **24**, 57.
- 8 B. Graham, L. Spiccia, G. D. Fallon, M. T. W. Hearn, F. E. Mabbs, B. Moubaraki and K. S. Murray, *J. Chem. Soc., Dalton Trans.*, 2002, 1226.
- 9 B. Graham, M. T. W. Hearn, P. C. Junk, C. M. Kepert, F. E. Mabbs, B. Moubaraki, K. S. Murray and L. Spiccia, *Inorg. Chem.*, 2001, **40**, 1536.
- 10 L. J. Farrugia, P. A. Lovatt and R. D. Peacock, *J. Chem. Soc., Dalton Trans.*, 1997, 911.
- 11 H. Weller, L. Siegfried, M. Neunberger, M. Zhender and T. A. Kaden, *Helv. Chim. Acta*, 1997, **80**, 2315.
- 12 S. J. Brudenell, L. Spiccia, D. C. R. Hockless and E. R. T. Tiekink, *Dalton Trans.*, 1999, 1475.
- 13 A. W. Addison, T. N. Rao, J. Reedijk, J. van Rijn and G. C. Verschoor, *J. Chem. Soc., Dalton Trans.*, 1984, 1349.
- 14 T. Tanase, J. W. Yun and S. J. Lippard, *Inorg. Chem.*, 1995, **34**, 4220.
- 15 H. Adams, D. Bradshaw and D. E. Fenton, *Polyhedron*, 2002, **21**, 1957.
- 16 S. R. Korupoju, N. Mangayarkarasi, P. S. Zacharias, J. Mizuthani and H. Nishihara, *Inorg. Chem.*, 2002, **41**, 4099.
- 17 H. Adams, D. Bradshaw and D. E. Fenton, *J. Chem. Soc., Dalton Trans.*, 2001, 3407.
- 18 W. N. Lipscomb and N. Sträter, *Chem. Rev.*, 1996, **96**, 2375; N. Sträter, W. N. Lipscomb, T. Klabunde and B. Krebs, *Angew. Chem., Int. Ed. Engl.*, 1996, **35**, 2025; D. E. Wilcox, *Chem. Rev.*, 1996, **96**, 2435.
- 19 J. L. Sessler, J. W. Sibert, A. K. Burrell and V. Lynch, *Inorg. Chem.*, 1993, **32**, 4277.
- 20 B. Graham, G. D. Fallon, M. T. W. Hearn, D. C. R. Hockless, G. Lazarev and L. Spiccia, *Inorg. Chem.*, 1997, **36**, 6366.
- 21 G. A. McLachlan, G. D. Fallon, R. L. Martin and L. Spiccia, *Inorg. Chem.*, 1995, **34**, 254.
- 22 B. J. Hathaway, in *Comprehensive Coordination Chemistry*, ed. G. Wilkinson, R. D. Gillard and J. A. McCleverty, Pergamon, Oxford, 1987, vol. 5, pp. 533–774 and references therein.
- 23 P. E. Kruger, B. Moubaraki, G. D. Fallon and K. S. Murray, *J. Chem. Soc., Dalton Trans.*, 2000, 713.
- 24 Y. Nishida and S. Kida, *J. Chem. Soc., Dalton Trans.*, 1986, 2633.
- 25 W. Mazurek, B. J. Kennedy, K. S. Murray, M. J. O'Connor, J. R. Rodgers, M. R. Snow, A. G. Wedd and P. R. Zwack, *Inorg. Chem.*, 1985, **24**, 3258.
- 26 K. Bertocello, G. D. Fallon, J. H. Hodgkin and K. S. Murray, *Inorg. Chem.*, 1988, **27**, 4750.
- 27 Y. Nishida, H. Shimo, H. Maehara and S. Kida, *J. Chem. Soc., Dalton Trans.*, 1985, 1945.
- 28 K. Wieghardt, I. Tolksdorf and W. Herrmann, *Inorg. Chem.*, 1985, **24**, 1230.
- 29 S. R. Hall, D. J. du Boulay and R. Olthof-Hazekamp (Editors), *The Xtal 3.7 System*, University of Western Australia, 2001.